Photosystem II

International Edition: DOI: 10.1002/anie.201502463
German Edition: DOI: 10.1002/ange.201502463

Resolving the Differences Between the 1.9 Å and 1.95 Å Crystal Structures of Photosystem II: A Single Proton Relocation Defines Two Tautomeric Forms of the Water-Oxidizing Complex**

Simon Petrie, Ron J. Pace, and Rob Stranger**

Abstract: *Great progress has been made in characterizing the water-oxidizing complex (WOC) in photosystem II (PSII) with the publication of a 1.9 Å resolution X-ray diffraction (XRD) and recently a 1.95 Å X-ray free-electron laser (XFEL) structure. However, these achievements are under threat because of perceived conflicts with other experimental data. For the earlier 1.9 Å structure, lack of agreement with extended X-ray absorption fine structure (EXAFS) data led to the notion that the WOC suffered from X-ray photoreduction. In the recent 1.95 Å structure, Mn photoreduction is not an issue, but poor agreement with computational models which adopt the 'high' oxidation state paradigm, has again resulted in criticism of the structure on the basis of contamination with lower S states of the WOC. Here we use DFT modeling to show that the distinct WOC geometries in the 1.9 and 1.95 Å structures can be straightforwardly accounted for when the Mn oxidation states are consistent with the 'low' oxidation state paradigm. Remarkably, our calculations show that the two structures are tautomers, related by a single proton relocation.*

The photosystem II (PSII) protein uses light to oxidize water to molecular oxygen and protons. This occurs within a Mn_4/Ca site, known as the water-oxidizing complex (WOC), through a series of intermediates (S states, $S_0 \ldots S_4$) of increasing mean Mn oxidation level.[1] The two substrate water molecules freely exchange with the site[2] up to S_3, with oxygen released in S_4. The stable, dark-adapted state is S_1, but the average metal cluster oxidation levels and individual Mn oxidation states are not resolved and, currently, the subject of controversy.[3]

XRD studies of PSII at progressively increasing resolution have been reported.[4] Those at 3.5, 3.0, and 2.9 Å resolution[4c,d,e] showed the positions of the Ca and Mn atoms in the WOC and the residues binding the metals. In 2011, Umena et al. reported a 1.9 Å structure of PSII, from material crystallized in the S_1 state. This advance resolved also the bridging oxo framework and coordinated water/hydroxide groups associated with the Mn_4Ca cluster of the WOC.[4f] However, it showed key differences between earlier EXAFS[5–7] and lower-resolution XRD data on PSII.[4e] Particular concerns were 1) the identity and position of the O5 group (see Figure 1) within the metal cluster of the WOC, and 2) the lengths of the "short" Mn1–Mn2 and Mn2–Mn3 distances.

In the 1.9 Å XRD data, O5 is weakly bound to four metals, Ca, Mn1, Mn3, and Mn4, at distances of 2.4 to 2.7 Å. As such, in this structure, O5 is unlikely to be an oxo or hydroxo group that ligates high-valent Mn, but could be a water molecule binding to Mn^{II} or Mn^{III} centers.

EXAFS studies[5–7,9] on the functional WOC have shown two Mn–Mn vectors of about 2.7 Å, in both S_1 and S_2. These are in accordance with Mn1–Mn2 and Mn2–Mn3 distances inferred in the earlier 2.9 Å XRD structure, but are significantly shorter than the analogous distances (2.8–2.9 Å) resolved in the 1.9 Å structure (Table 1). This discrepancy led to suggestions that the Mn–Mn distances in the 1.9 Å structure are distorted (lengthened) through X-ray photoreduction.[8,9]

Table 1: Key distances from extended-range EXAFS studies,[7,9] and the 1.9 Å[4f] XRD and 1.95 Å[4h] XFEL structure determinations for PSII by Shen et al., compared with model geometries from our earlier[10] and current DFT calculations.

Parameter [Å][a]	EXAFS[b]	XRD[c] 1.9 Å	Calc.[10]	XFEL[c] 1.95 Å	Calc[d]
r[Mn1–Mn2]	2.72, 2.73	2.84	2.90	2.70	2.72
r[Mn2–Mn3]	2.72, 2.71	2.89	2.89	2.71	2.81
r[Mn1–Mn3]	3.20, 3.19	3.29	3.42	3.25	3.33
r[Mn3–Mn4]	2.83, 3.03	2.97	3.03	2.87	2.85
r[Mn1–Mn4]		5.00	5.09	4.92	4.84
r[Ca–Mn1]		3.51	3.38	3.50	3.44
r[Ca–Mn2]	3.40, 3.34	3.36	3.18	3.34	3.36
r[Ca–Mn3]		3.41	3.48	3.44	3.69
r[Ca–Mn4]		3.80	3.82	3.74	3.81
r[O5–Mn1]		2.60	2.64	2.70	2.66
r[O5–Mn3]		2.38	2.61	2.26	2.37
r[O5–Mn4]		2.50	2.60	2.35	2.28
r[O5–Ca]		2.50	2.71	2.51	2.44

[a] Refer to Figure 1 for Mn atom ordering. [b] Values from specific models IIc[7] and C-III,[9] respectively (see main text). [c] Average of monomer A refinements. [d] Present calculations, average from models S1 a and S1 b, Supporting Information.

[*] Dr. S. Petrie, Prof. R. J. Pace, Prof. R. Stranger
Research School of Chemistry, Australian National University
Canberra ACT 0200 (Australia)
E-mail: ron.pace@anu.edu.au
rob.stranger@anu.edu.au

[**] R.S. and R.J.P. gratefully acknowledge financial assistance from the Australian Research Council. The authors also acknowledge the generous provision of supercomputing time on the platforms of the NCI (National Computational Infrastructure) Facility in Canberra, Australia, which is supported by the Australian Commonwealth Government. We also thank Richard Terrett for assistance in the preparation of the manuscript figures. We also acknowledge financial support from Tianjin EDBA Technology Development Com. Ltd.

Supporting information for this article is available on the WWW under http://dx.doi.org/10.1002/anie.201502463.

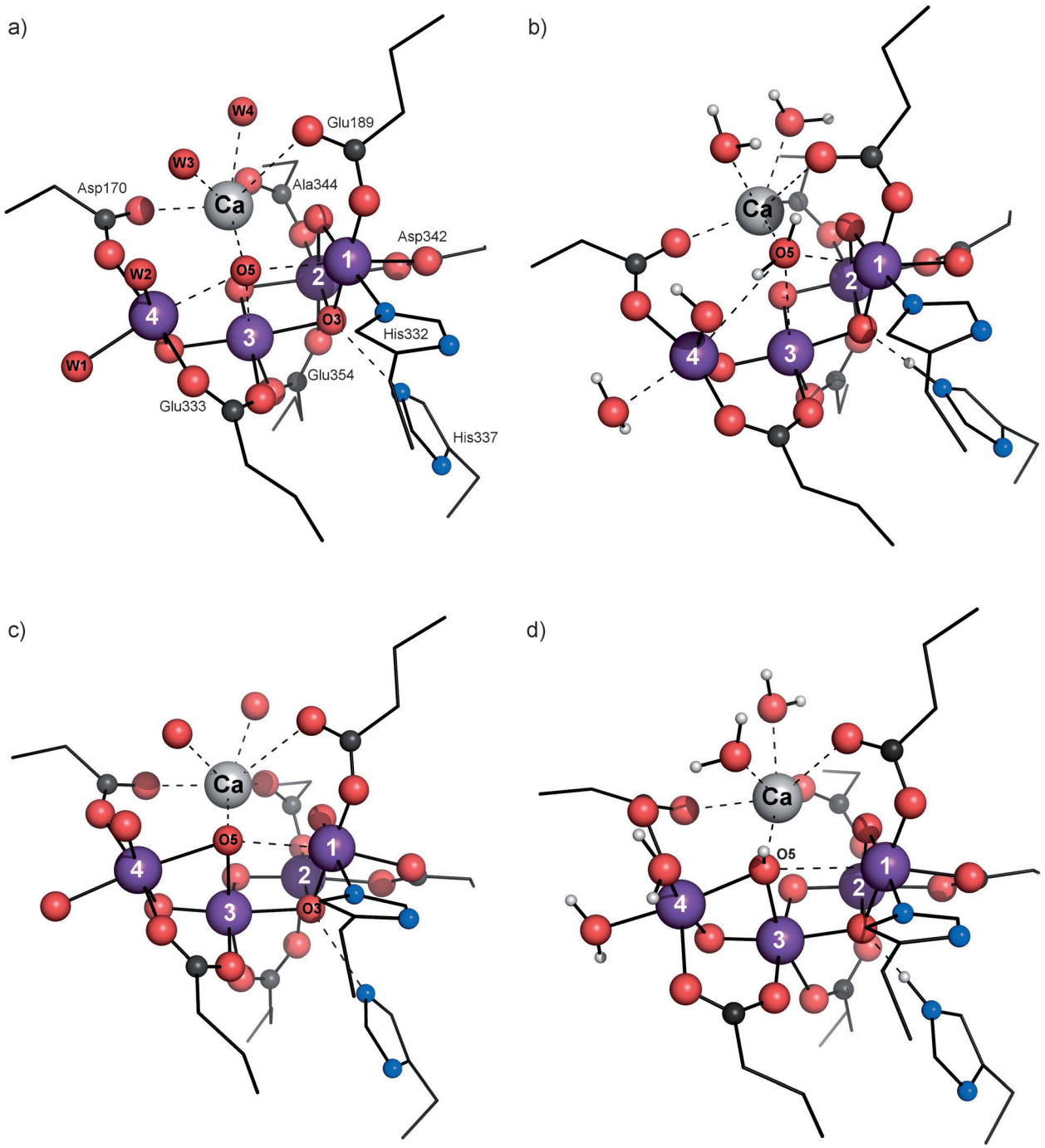

Figure 1. XRD WOC structures at a) 1.9 Å and c) 1.95 Å. Our corresponding optimized models are shown in (b) and (d), respectively (complete optimized 1.95 Å model in the Supporting Information, Figure S1). Experimental Mn–Mn distances and W2/O5 positions are well reproduced in both models. In b) W2 is OH^- and O5 is H_2O; in d) W2 is H_2O and O5 is OH^-. Structures (b) and (d) are tautomers with identical total charge (0) and mean Mn oxidation state (+3.0) but different Mn oxidation state sequences, III,III,III,III and III,IV,III,II for Mn1 to Mn4, respectively.

Suga et al. have now reported a 1.95 Å resolution structure,[4h] using a pulsed XFEL source and multiple crystals, with X-ray dosages unlikely to induce Mn photoreduction. The new structure is broadly similar to the earlier one, but with some key differences (Table 1). The Mn1–Mn2 and Mn2–Mn3 distances are shorter, around 2.7 Å, close to the EXAFS and the inferred 2.9/3.0 Å XRD values. O5 still weakly binds to the same four metals, but is now closer to Mn3 and Mn4, bridging these at distances of about 2.3 Å. Notably, *r*(Mn3–Mn4) is still relatively "long" (≈2.9 Å) and the Mn–O5 distances (2.2–2.7 Å) remain too long for O5 to be other than a water molecule or hydroxide.

The most detailed EXAFS studies on S_1 originate from extended-range X-ray back-scattering measurements (16–17 $Å^{-1}$),[7,9] including results from ordered samples.[7] Metal distances obtained from two optimal fitting models with Mn

assignments consistent with the latest 1.95 Å XFEL structure, are shown in Table 1. The EXAFS data are in excellent agreement with each other and also the 1.95 Å XFEL results.

Superficially, distortion of the WOC through X-ray exposure is supported by the longer Mn–Mn distances in the 1.9 Å structure. However, separate A and B monomer refinements in the dimeric PSII crystals were obtained,[4f,g] which is unlikely if the "distortions" arise from random X-ray photoreduction. Furthermore, this has been tested experimentally[11] using Mn EXAFS to monitor the X-ray exposure regimes used by Umena et al. in 2011.[4f] These studies (in particular, see discussions by Vinyard et al.[12]) showed that for X-ray dosage equivalent to the average exposure in the Umena et al. data, approximately 60% of the initial 2.7 Å EXAFS scattering peak intensity remained and no conversion into 2.8–2.9 Å Mn–Mn vector(s) was observed. Photoreduced sites lost all well-resolved local structure and presumably contributed only to diffuse (background) or low-resolution scattering. Thus, the suggestion that the detailed features of the original[4f,g] high-resolution structure of Umena et al. arise from Mn photoreduction totally lacks independent experimental justification. The explanation must lie elsewhere.

Density functional theory (DFT) has been extensively applied to the WOC.[8,10,13,14] These studies must assume a mean oxidation level for the Mn ions well above +2.0 from spectroscopic data. There are two alternatives, the 'low' and 'high' oxidation state paradigms, with S_1 levels of +3.0 and +3.5, respectively. Most groups have favored the high-oxidation state paradigm, mainly from spectroscopic interpretation (principally XANES, EPR)[13] based on model Mn–oxo systems, never precise analogues of the actual Mn environment of the WOC. We have shown, using time-dependent DFT, that when the metal–ligand environments are properly accounted for, the Mn XANES data are most consistent with the low oxidation state paradigm.[14b,c] Re-examination of other spectroscopic data also supports this observation.[3b]

The low oxidation state paradigm is also clearly supported by electron counting when the functional enzyme is photo-assembled from apo-protein and four Mn^{II} ions, as shown by Dismukes et al.[15] Last, pulsed EPR studies on the S_2 state at 2.5 K by Jin et al.[16] observed at least two centers with large ^{55}Mn nuclear hyperfine anisotropy associated with Mn^{III} ions, consistent only with the low-oxidation-state model (i.e. $Mn^{III}_3Mn^{IV}$ in S_2). The spin projection coefficients, ρ_i, for the Mn centers were of unexpected magnitude, with $\rho_1 \approx 2$, $\rho_2 \approx -1$, and ρ_3 and ρ_4 both small and approximately cancelling, as Mn3 and Mn4 are in the same oxidation state. The same outcome was reached in a recent high-level computational study of the OEC.[17]

To address the WOC geometries seen in EXAFS, and the 1.9 and 2.9 Å crystal structures, we previously undertook large-scale (≈200 atom) DFT modeling of the WOC region.[10] The results for the 1.9 Å structure are compared with the corresponding XRD region in Figure 1 a,b, with key interatomic distances in Table 1. The calculated and experimental values match well, particularly the anomalous Mn1–Mn2 and Mn2–Mn3 vectors, previously thought to arise from X-ray photoreduction. This occurs because the preferred low oxidation state S_1 redox pattern for the 1.9 Å structure is III,III,III,III (Mn1 to Mn4), causing Jahn–Teller "frustration" at the μ_3-oxo bridge (O3) connecting Mn1, Mn2, and Mn3, and elongation of the Mn1–Mn2 and Mn2–Mn3 distances.[10] The $(Mn^{III})_4$ configuration occurs only because a proton is relocated from the W2 water molecule on Mn4 to the τN on His337, thus allowing hydrogen bonding to the μ_3-oxo bridge, as seen in the 1.9 Å XRD structure (Figure 1 a). This and other relocations are presumed to arise through differences in the chemical workup preceding crystallography. It does not necessarily imply that direct proton transfer from W2 to His337, even mediated by "background" water molecules, could normally occur "functionally". This particular hydrogen bonding interaction is absent in the 2.9 Å structure, as His337 is not oriented toward the inferred position of the μ_3-oxo bridge and W2 remains a water molecule. Computationally, the S_1 redox pattern becomes III,IV,III,II in the 2.9 Å structure and the Mn1–Mn2 and Mn2–Mn3 distances are now shorter (≈2.7 Å), as seen in the EXAFS.

The WOC regions of the 1.90 and 1.95 Å structures (Figure 1 a,c) show important similarities and differences. Both retain the His337−O3 hydrogen bond, indicating His337 protonation. In the 1.95 Å structure, this proton cannot come from W1 or W2 on Mn4, as calculations then predict a redox pattern of $(Mn^{III})_4$, with "long" (≈2.9 Å) Mn1–Mn2 and Mn2–Mn3 distances. However, O5 has moved significantly closer to Mn3 and Mn4 in the 1.95 Å structure (Table 1), apparently bridging these metals. Thus O5, modeled as a water molecule in the 1.9 Å structure, has likely become a hydroxide group in the 1.95 Å structure, with a proton relocated to His337.

Our computational WOC models for the 1.9 and 1.95 Å structures are shown in Figure 1 b,d. The 1.9 Å model derives from our earlier study,[10] with W2 deprotonated, giving a $(Mn^{III})_4$ redox pattern as discussed above. For the 1.95 Å model, O5 is a hydroxide and W2 a water molecule; with a calculated redox pattern of III,IV,III,II (as for the 2.9 Å structure). Remarkably, the differences in the Mn cluster geometries between the 2.9, 1.9, and 1.95 Å crystal structures can all be rationalized in the low-oxidation-state model simply through the single proton relocations shown in Figure 2 B.

Figure 2 A shows the Mn3 and Mn4 centers and key ligating groups. It is this region which most differentiates the high and low oxidation state S_1 structures. The XRD data are compared with our models for the 2.9 Å (no proton relocation to His337), 1.9 Å (proton relocated from W2 to His337) and 1.95 Å structures (proton relocated from O5 to His337). Our modeling reproduces virtually all key protonation and Mn redox-sensitive structural features, including the Mn3–Mn4 distance contraction, going from the 2.9 to 1.95 Å structures, the Mn4–W1/W2 bond lengths, where resolved, and crucially, the Mn3/Mn4–O5 bond lengths. These distances have always challenged high oxidation state models[3,13] (Supporting Information, Figure S2), in which O5 is either an oxo or hydroxo group bound to Mn^{III} or Mn^{IV}, with computed Mn−O bond lengths typically smaller than 1.9 Å and Mn3–Mn4 distances smaller than 2.8 Å. W1 and W2 are also generally not water molecules, with computed Mn–O distances of less

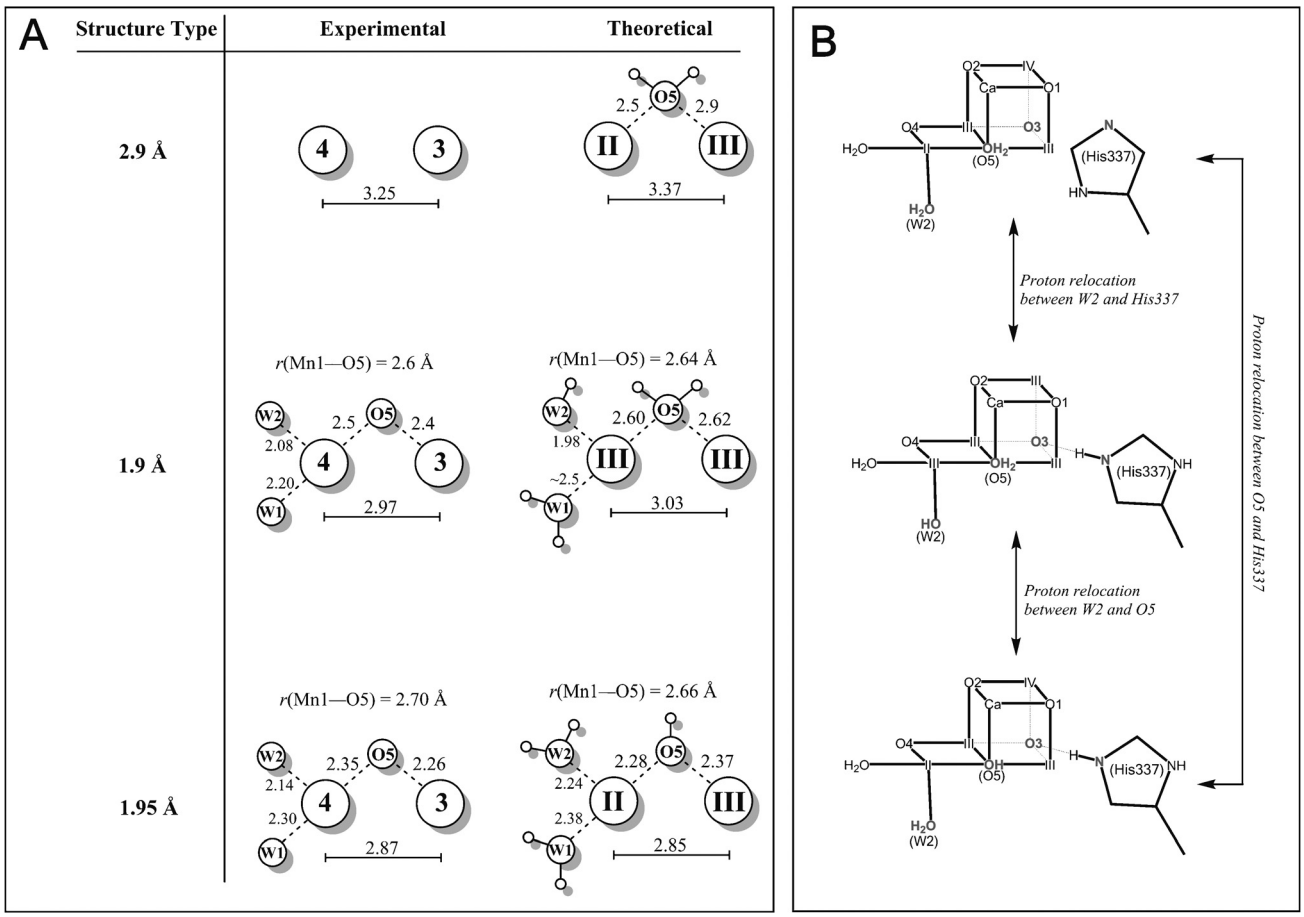

Figure 2. Comparison of the 2.9, 1.9, and 1.95 Å WOC structural features. Section A) Mn3/Mn4 region, with geometries and Mn oxidation states from our computational models (Ref. [10] and present work). Section B) Tautomeric relationships and S_1 Mn-oxidation-state patterns, applying for the models.

than 2.0 Å. While Mn photoreduction could previously be invoked to rationalize these discrepancies, this is no longer credible with the 1.95 Å structure. Ironically, this structure, which promised to "validate" the high oxidation state models through its "short" Mn1–Mn2 and Mn2–Mn3 distances, in fact condemns them through its geometry around Mn3 and Mn4. Indeed, recent computational studies of the WOC favoring the high oxidation state paradigm, were forced to discount the 1.95 Å structure because of poor agreement with their models, instead suggesting that the XFEL data comprised a mixture of S_0 and S_1 states.[13f,g] In contrast with our results, one of these studies[13f] argued that their low oxidation state models were in even worse agreement with the XFEL data. However, the discrepancy arises from their modeling of O5 as an oxo rather than a hydroxo group, and O3 and O4 also as hydroxides. As a result, their low oxidation state assignments for S_1 were either IV,III,III,II or III,III,IV,II, for Mn1 to Mn4, respectively, rather than our scheme of III,IV,III,II.

Table 1 shows that our calculations quantitatively capture the key differences between the 1.9 and 1.95 Å structures. Our 1.95 Å low oxidation state model reproduces the contentious Mn1–Mn2, Mn2–Mn3 and Ca/Mn–O5 distances, with root mean square deviation (RMSD) for the M–M and M–O distances of 0.086 Å (0.065 Å for the set of 'short' XFEL distances; see the Supporting Information). Our best high oxidation state model gives distinctly poorer performance (corresponding RMSD values 0.164 and 0.134 Å).

From Table 1 and Figure 2, including conclusions from our recent review of WOC spectroscopy[3b] and the photoassembly results of Kolling et al.,[15] it is difficult to imagine how the WOC oxidation states could be different from the ones we propose. Further, the exchange kinetics[2] of the substrate waters are too facile throughout the S-state cycle to plausibly involve anything other than bound water molecules, up to and including S_3.[2b] This is readily achievable in the low oxidation state paradigm[18] (O5 is one of them), but not in high oxidation state models, as the substrates must generally deprotonate progressively throughout the S-state cycle.[13a,f]

Keywords: density functional calculations · manganese · photosystem II · water-oxidizing complex · water splitting

How to cite: *Angew. Chem. Int. Ed.* **2015**, *54*, 7120–7124
Angew. Chem. **2015**, *127*, 7226–7230

[1] K. Satoh, T. Wydrzynski, Govindjee, *Photosystem II: The Light Driven Water: Plastoquinone Oxidoreductase*, Springer, Dordrecht, The Netherlands, **2005**, pp. 11–22.
[2] a) W. Hillier, T. Wydrzynski, *Biochim. Biophys. Acta Bioenerg.* **2001**, *1503*, 197–209; b) R. J. Pace, K. A. Åhrling, *Biochim. Biophys. Acta Bioenerg.* **2004**, *1655*, 172–178.

[3] a) P. Gatt, R. Stranger, R. J. Pace, *J. Photochem. Photobiol. B* **2011**, *104*, 80 – 93; b) R. J. Pace, L. Jin, R. Stranger, *Dalton Trans.* **2012**, *41*, 11145 – 11160.
[4] a) A. Zouni, H.-T. Witt, J. Kern, P. Fromme, N. Krauss, W. Saenger, P. Orth, *Nature* **2001**, *409*, 739 – 743; b) N. Kamiya, J.-R. Shen, *Proc. Natl. Acad. Sci. USA* **2003**, *100*, 98 – 103; c) K. N. Ferreira, T. M. Iverson, K. Maghlaoui, J. Barber, S. Iwata, *Science* **2004**, *303*, 1831 – 1838; d) B. Loll, J. Kern, W. Saenger, A. Zouni, J. Biesiadka, *Nature* **2005**, *438*, 1040 – 1044; e) A. Guskov, J. Kern, A. Gabdulkhalov, M. Broser, A. Zouni, W. Saenger, *Nat. Struct. Mol. Biol.* **2009**, *16*, 334 – 342; f) Y. Umena, K. Kawakami, J.-R. Shen, N. Kamiya, *Nature* **2011**, *473*, 55 – 60; g) H. M. K. Koua, Y. Umena, K. Kawakami, J.-R. Shen, *Proc. Natl. Acad. Sci. USA* **2013**, *110*, 3889 – 3894; h) M. Suga, F. Akita, K. Hirata, G. Ueno, H. Murakami, Y. Nakajima, T. Shimizu, K. Yamashita, M. Yamamoto, H. Ago, J.-R. Shen, *Nature* **2015**, *517*, 99 – 103.
[5] M. Haumann, C. Müller, P. Liebisch, L. Iuzzolino, J. Dittmer, M. Grabolle, T. Neisius, W. Meyer-Klaucke, H. Dau, *Biochemistry* **2005**, *44*, 1894 – 1908.
[6] a) J. Yano, Y. Pushkar, P. Glatzel, A. Lewis, K. Sauer, J. Messinger, U. Bergmann, V. Yachandra, *J. Am. Chem. Soc.* **2005**, *127*, 14974 – 14975; b) J. Yano, J. Kern, K.-D. Irrgang, M. J. Latimer, U. Bergmann, P. Glatzel, Y. Pushkar, J. Biesiadka, B. Loll, K. Sauer, J. Messinger, A. Zouni, V. K. Yachandra, *Proc. Natl. Acad. Sci. USA* **2005**, *102*, 12047 – 12052.
[7] Y. Pushkar, J. Yano, P. Glatzel, J. Messinger, A. Lewis, K. Sauer, U. Bergmann, V. Yachandra, *J. Biol. Chem.* **2007**, *282*, 7198 – 7208.
[8] a) S. Luber, I. Rivalta, Y. Umena, K. Kawakami, J.-R. Shen, N. Kamiya, G. W. Brudvig, V. Batista, *Biochemistry* **2011**, *50*, 6308 – 6311; b) P. E. M. Siegbahn, *ChemPhysChem* **2011**, *12*, 3274 – 3280; c) W. Ames, D. A. Pantazis, V. Krewald, N. Cox, J. Messinger, W. Lubitz, F. Neese, *J. Am. Chem. Soc.* **2011**, *133*, 19743 – 19757; d) A. Galstyan, A. Robertazzi, E. W. Knapp, *J. Am. Chem. Soc.* **2012**, *134*, 7442 – 7449.
[9] A. Grundmeier, H. Dau, *Biochim. Biophys. Acta Bioenerg.* **2012**, *1817*, 88 – 105.
[10] P. Gatt, S. Petrie, R. Stranger, R. J. Pace, *Angew. Chem. Int. Ed.* **2012**, *51*, 12025 – 12028; *Angew. Chem.* **2012**, *124*, 12191 – 12194.
[11] a) C. Glöckner, J. Kern, M. Broser, A. Zouni, V. Yachandra, J. Yano, *J. Biol. Chem.* **2013**, *288*, 22607 – 22620; b) M. Grabolle, M. Haumann, C. Müller, P. Liebisch, H. Dau, *J. Biol. Chem.* **2006**, *281*, 4580 – 4588.
[12] D. J. Vinyard, G. M. Ananyev, G. C. Dismukes, *Annu. Rev. Biochem.* **2013**, *82*, 577 – 606.
[13] a) P. E. M. Siegbahn, *Phys. Chem. Chem. Phys.* **2012**, *14*, 4849 – 4856; b) M. Kusunoki, *J. Photochem. Photobiol.* **2011**, *104*, 100 – 110; c) T. Saito, S. Yamanaka, K. Kanda, H. Isobe, Y. Takano, Y. Shigeta, Y. Umena, K. Kawakami, J.-R. Shen, N. Kamiya, M. Okumura, M. Shoji, Y. Yoshioka, K. Yamaguchi, *Int. J. Quantum Chem.* **2012**, *112*, 253 – 276; d) S. Yamanaka, T. Saito, K. Kanda, H. Isobe, Y. Umena, K. Kawakami, J.-R. Shen, N. Kamiya, M. Okumura, H. Nakamura, K. Yamaguchi, *Int. J. Quantum Chem.* **2012**, *112*, 321 – 343; e) D. A. Pantazis, W. Ames, N. Cox, W. Lubitz, F. Neese, *Angew. Chem. Int. Ed.* **2012**, *51*, 9935 – 9940; *Angew. Chem.* **2012**, *124*, 10074 – 10079; f) V. Krewald, M. Retegan, N. Cox, J. Messinger, W. Lubitz, S. DeBeer, F. Neese, D. A. Pantazis, *Chem. Sci.* **2015**, *6*, 1676 – 1695; g) M. Askerka, D. J. Vinyard, J. Wang, G. W. Brudvig, V. S. Batista, *Biochemistry* **2015**, *54*, 1713 – 1716.
[14] a) S. Petrie, P. Gatt, R. Stranger, R. J. Pace, *Phys. Chem. Chem. Phys.* **2012**, *14*, 4651 – 4657; b) A. R. Jaszewski, R. Stranger, R. J. Pace, *Phys. Chem. Chem. Phys.* **2009**, *11*, 5634 – 5642; c) A. R. Jaszewski, S. Petrie, R. J. Pace, R. Stranger, *Chem. Eur. J.* **2011**, *17*, 5699 – 5713; d) S. Petrie, P. Gatt, R. Stranger, R. J. Pace, *Phys. Chem. Chem. Phys.* **2012**, *14*, 11333 – 11343; e) R. J. Pace, R. Stranger, S. Petrie, *Dalton Trans.* **2012**, *41*, 7179 – 7189; f) R. Terrett, S. Petrie, R. J. Pace, R. Stranger, *Chem. Commun.* **2014**, *50*, 3187 – 3190; g) S. Petrie, R. J. Pace, R. Stranger, *Chem. Eur. J.* **2015**, *21*, 6780 – 6792.
[15] D. R. J. Kolling, N. Cox, G. M. Ananyev, R. J. Pace, G. C. Dismukes, *Biophys. J.* **2012**, *103*, 313 – 322.
[16] L. Jin, P. Smith, C. J. Noble, R. Stranger, G. R. Hanson, R. J. Pace, *Phys. Chem. Chem. Phys.* **2014**, *16*, 7799 – 7812.
[17] Y. Kurashige, G. K.-L. Chan, T. Yanai, *Nat. Chem.* **2013**, *5*, 660 – 666.
[18] S. Petrie, R. Stranger, R. J. Pace, *Angew. Chem. Int. Ed.* **2010**, *49*, 4233 – 4236; *Angew. Chem.* **2010**, *122*, 4329 – 4332.

Received: March 17, 2015
Published online: April 27, 2015

